

# Validation of KREAM Based on *In-Situ* Measurements of Aviation Radiation in Commercial Flights

Junga Hwang<sup>1,2†</sup>, Jaeyoung Kwak<sup>1,2</sup>, Gyeongbok Jo<sup>3</sup>, Uk-won Nam<sup>1</sup>

<sup>1</sup>Korea Astronomy and Space Science Institute, Daejeon 34055, Korea

<sup>2</sup>Department of Astronomy and Space Science, Korea University of Science and Technology, Daejeon 34113, Korea

<sup>3</sup>Department of Astronomy and Space Science, Chungnam National University, Daejeon 34134, Korea

There has been increasing necessity of more precise prediction and measurements of aviation radiation in Korea. For our air crew and passengers' radiation safety, we develop our own radiation prediction model of KREAM. In this paper, we validate the KREAM model based on comparison with Liulin observations. During early three months of this year, we perform total 25 experiments to measure aviation radiation exposure using Liulin-6K in commercial flights. We found that KREAM's result is very well consistent with Liulin observation in general. NAIRAS shows mostly higher results than Liulin observation, while CARI-6M shows generally lower results than the observations. The percent error of KREAM compared with Liulin observation is 10.95%. In contrast, the error for NAIRAS is 43.38% and 22.03% for CARI-6M. We found that the increase of the altitude might cause sudden increase in radiation exposure, especially for the polar route. As more comprehensive and complete analysis is required to validate KREAM's reliability to use for the public service, we plan to expand these radiation measurements with Liulin and Tissue Equivalent Proportional Counter (TEPC) in the near future.

**Keywords:** space radiation, KREAM, Liulin

## 1. INTRODUCTION

Aviation radiation is an unavoidable space weather phenomenon. In Korea, the Environmental Radiation Safety Control Act regulates the annual dose limit for the aircrew. Radiation in commercial airplanes' altitude is the ionizing radiation originated from the primary protons of galactic cosmic rays (GCR) and solar energetic particles (SEP). It is discovered that accumulated radiation exposure is caused by high linear energy transfer (LET) of those incident energetic particles into the Earth's atmosphere (Wilson et al. 2005). Radiation by GCR is relatively stable and does not change much. That by SEP is somewhat transient and increasing suddenly with solar activities such as solar flare and coronal mass ejection. So, the resultant aviation radiation exposure is the combination of two main contributions from both GCR and SEP origins. At

commercial flight altitude, aviation radiation is the latitude, altitude, and solar activity function. Earth's magnetic field cuts off the energetic incident particles depending on the latitude. The cutoff rigidity is relatively higher in the equator than the polar region, and the energetic particles can precipitate easily through the polar region.

International Commission on Radiological Protection (ICRP) and International Commission on Radiation Units and measurements (ICRU) have recommended to predict aviation radiation exposure for the air crew's radiation safety. To satisfy this purpose, various estimation programs such as Sievert, EPCARD, PCaire, and JISCARD were developed, the Federal Aviation Administration (FAA) distributes the CARI-6/6M computer program (O'Brien et al. 2003), and NASA also developed the NAIRAS program (Mertens et al. 2013). While CARI-6/6M considers the GCR contribution, the NAIRAS program considers both the GCR and SEP

© This is an Open Access article distributed under the terms of the Creative Commons Attribution Non-Commercial License (<https://creativecommons.org/licenses/by-nc/3.0/>) which permits unrestricted non-commercial use, distribution, and reproduction in any medium, provided the original work is properly cited.

Received 06 NOV 2020 Revised 25 NOV 2020 Accepted 26 NOV 2020

† Corresponding Author

Tel: +82-42-865-2061, E-mail: jahwang@kasi.re.kr

ORCID: <https://orcid.org/0000-0002-6862-5854>

effects. Currently, FAA develops an updated version of CARI-7 and -7A, including the SEP events. We also develop by ourselves the Korean Radiation Exposure Assessment model for the aviation route dose (KREAM) for radiation safety of the Korean aircrew and passengers (Hwang et al. 2010, 2014). Most advanced countries have their aviation radiation assessment program to assess the aviation radiation exposure of the aircrew and the passengers, and they have continued updating their own programs.

In this paper, we compare the *in-situ* measurements by using Liulin-6K equipment at the commercial flights with KREAM results to validate the reliability of our aviation radiation prediction model KREAM. We also compare the measurements with the other two models of CARI-6M and NAIRAS. Aviation radiation measurements were performed during the early three months of 2020. Liulin-6K equipment used for our study was initially designed to measure an absorbed dose and a significant dose of space astronauts. Liulin type equipment using a silicon sensor to detect the charged particles' LET has been continuously improved since it was firstly used in 1988 for the MIR space station (Dachev et al. 2015). Its measurements are known to be reliable not only in space but also in aviation altitude over the polar route (Hwang et al. 2010). This year is the solar

minimum period connecting the solar cycle 24 and 25, so it is very proper to verify in-situ data and program because the values are comparably stable than the solar maximum period. Undoubtedly more comprehensive verification of the KREAM program should be performed in the future.

## 2. EXPERIMENTS

The experiments were carried out 25 times from March 11 to May 26 of 2020. Table 1 indicates the flight information of departure time, arrival time, flight time, departure airport, arrival airport, and maximum altitude for each experiment. Most flights start from or return to Incheon airport (ICN). The flights cover various continents of North America, South-east Asia, Australia, Russia, and Europe. Flight times are written in Universal Time (UT). We can get the GPS information of each route from a flight aware web site (<https://flightaware.com>). The site offers rough information about air routes for the permitted commercial flights. These geographical data from the web site are critically important, even though some geographic data points are missing. These data gaps were extrapolated to get the continuous flight information of latitude, longitude, and altitude required

**Table 1.** Summarized flight information for aviation route dose measurements

	date	Universal time (UT)		Flight time	Departure airport	Arrival airport	Maximum altitude (km)
		Departure	Arrival (*next day)				
1	03/11	02:17	13:49	11 h 32 m	ICN	FRA	10.98
2	03/13	17:31	03:10*	9 h 39 m	FRA	ICN	10.71
3	03/18	01:11	14:16	13 h 5 m	ICN	JFK	10.67
4	03/20	17:35	07:22*	13 h 47 m	JFK	ICN	10.39
5	03/22	01:57	13:51	11 h 54 m	ICN	ORD	10.68
6	03/24	17:43	07:32*	13 h 49 m	ORD	ICN	10.97
7	04/01	17:49	04:09*	10 h 20 m	ICN	VIE	10.37
8	04/04	06:30	08:36	2 h 6 m	VIE	OSL	8.53
9	04/04	10:50	19:42	8 h 52 m	OSL	ICN	10.71
10	04/10	01:10	10:42	9 h 32 m	BNE	ICN	10.97
11	04/15	10:44	21:34	10 h 50 m	ICN	LAX	11.28
12	04/17	06:48	18:54	12 h 6 m	LAX	ICN	10.97
13	04/23	00:35	13:29	12 h 54 m	ICN	ATL	11.29
14	04/25	16:35	07:22*	14 h 47 m	ATL	ICN	11.62
15	04/28	23:46	08:29*	8 h 43 m	ICN	SVO	10.98
16	04/29	10:59	13:45	2 h 46 m	SVO	FRA	10.97
17	05/01	16:27	02:11*	9 h 44 m	FRA	ICN	10.68
18	05/05	12:26	22:52	10 h 26 m	ICN	LAX	11.28
19	05/08	01:11	13:37	12 h 26 m	LAX	ICN	11.59
20	05/15	03:53	15:23	11 h 30 m	ICN	FRA	10.97
21	05/16	17:41	03:44*	9 h 57 m	FRA	ICN	11.28
22	05/20	09:50	14:35	4 h 45 m	ICN	SGN	11.89
23	05/20	16:45	21:20	4 h 35 m	SGN	ICN	12.50
24	05/24	23:48	13:17*	13 h 29 m	ICN	JFK	11.28
25	05/26	15:52	06:46*	14 h 54 m	JFK	ICN	11.59

to run the KREAM model. Using a globally effective dose map originally implemented inside the KREAM program package, the route dose can be produced precisely for each specific flight.

Table 2 shows that the route dose and averaged dose rate are measured by Liulin-6K and geographic information of maximum altitude and latitude for 25 flights. Liulin spectrometer’s primary purpose is continued monitoring of doses, fluxes, and spectra during aircraft flights. The spectrometer can work by internal Li-Ion batteries. Liulin-6K is a kind of energy deposition spectrometer using a silicon sensor. These semiconductor detectors cannot measure the effective dose directly but can obtain the ambient dose equivalent  $H^*(10)$  from the deposited energy in the detector (Green et al. 2005; Spurný 2005; Ploc et al. 2011; Kubančák et al. 2014). The reliability of this conversion method has been verified from numerous previous measurements. But there remains a fundamental limitation caused by the charge sensitive detector of the Si sensor. To solve this problem, we are currently developing a Tissue-Equivalent Proportional Counter (TEPC) equipment, which considers biological effects more sophisticatedly (Malimban et al. 2019). The tissue equivalence principle is based on the fact that the significant parameter in radiation energy

transfer is the atomic composition of traversing material.

In contrast, the chemical combination of material elements is not essential. Therefore, human tissue can be replaced with substance providing the same as tissue energy-absorbing properties. Such materials are usually a mixture of hydrogen, carbon, nitrogen, and oxygen. One of these mixtures is A-150 plastic commonly used for the wall of a tissue-equivalent proportional counter. The Counter’s chamber is filled with methane or propane-based tissue-equivalent gas. Further experiments using our TEPC are planned to be carried out soon.

### 3. ANALYSIS

#### 3.1 *In-Situ* Observation Data Using Liulin-6K

We classified the experiments depending on continents to show the correlation between route dose and geographic information such as flight time, latitude, and altitude. In Table 2, in the case of North-America, a cumulative effective route dose of flights to ICN (from #7 to #12) is 557.02  $\mu$ Sv, which is greater about 15% than that of flights from ICN (from #1 to #6) whose amount is 470.97  $\mu$ Sv. That difference

**Table 2.** Route dose, averaged dose rate, maximum altitude, and maximum latitude measured by Liulin-6K depending on continents

		Departure airport	Arrival airport	Route dose ( $\mu$ Sv)	Averaged dose rate ( $\mu$ Sv/hr)	Maximum altitude (km)	Maximum latitude (degree)
North America	1	ICN	JFK	102.82	7.86	10.67	63.90
	2	ICN	JFK	75.50	5.60	11.28	48.51
	3	ICN	ORD	80.60	6.77	10.68	60.53
	4	ICN	LAX	54.36	5.02	11.28	43.16
	5	ICN	LAX	62.04	5.95	11.28	48.00
	6	ICN	ATL	95.65	7.41	11.29	51.16
	7	JFK	ICN	84.00	6.10	10.39	84.57
	8	JFK	ICN	113.73	7.63	11.59	61.42
	9	ORD	ICN	81.79	5.92	10.97	61.29
	10	LAX	ICN	70.72	5.84	10.97	58.73
	11	LAX	ICN	90.05	7.24	11.59	57.23
	12	ATL	ICN	116.73	7.90	11.62	83.53
Europe	13	ICN	FRA	61.32	5.32	10.98	56.26
	14	ICN	FRA	83.95	7.30	10.97	61.82
	15	ICN	VIE	52.44	5.08	10.37	56.26
	16	ICN	SVO	55.59	6.38	10.98	60.14
	17	FRA	ICN	56.50	5.85	10.71	60.11
	18	FRA	ICN	55.51	5.71	10.68	61.80
	19	FRA	ICN	67.87	6.82	11.28	59.59
	20	OSL	ICN	47.18	5.32	10.71	62.19
	21	SVO	FRA	15.46	5.58	10.97	55.97
	22	VIE	OSL	6.10	2.90	8.53	60.41
Australia, Southeast Asia	23	ICN	SGN	11.16	2.35	11.89	37.58
	24	BNE	ICN	25.19	2.64	10.97	37.44
	25	SGN	ICN	10.96	2.39	12.50	37.46

is undoubtedly caused by the difference in flight time. The total flight time of return flights to ICN is 81.8 hours, which is longer about 11% than that of departure flights from ICN, which is 72.6 hours. The time difference is due to the jet stream because the jet stream, which rotates the Earth in a counter-clockwise direction from the top view, pushes or pulls aircraft (Irvine et al. 2016). All return flights to ICN (from #7 to #12) flew above the latitude of 55 degrees, and 50% of these flights (three flights) flew over the altitude of 11.5 km (about 38,000 feet). This is contrasted from the results of departure flights from ICN; there are just two flights out of six flights that flew over the latitude of 55 degrees, and none of these six flights flown over the altitude of 11.5 km.

In the case of Europe, total route doses of departure and return flights are 253.30  $\mu\text{Sv}$  and 227.06  $\mu\text{Sv}$ , and respectively, the former is more significant, about 11% than the latter. It is also caused by the flight time difference. In this case, the total flight time of departure and return flights is 42.08 hours and 38.2 hours. The difference is about 10%. Also, the latitude and longitude are similar in both the 13th and the 15th flights. The mean effective dose rate of the 13th flight is much higher than the 15th flight because the altitude of the 13th flight is much higher than that of the 15th flight. On the other hand, for the 13th and 14th flight, their averaged dose rates differ about 2  $\mu\text{Sv/hr}$  despite the similar maximum latitude. The difference could be interpreted as caused by the difference in flight altitudes. For the 17th and the 21st flights, although the 21st flight flew at high latitude overall, the averaged dose rate is lower than that of the 17th, which flew at low latitude but partially reached higher latitude. It might be explained if flying latitude exceeds a certain threshold, the effective dose might ascend rapidly.

Fig. 1 shows the relative influence of altitude and latitude on an effective dose rate. The X-axis of Fig. 1 is maximum altitude (km), the Y-axis is maximum latitude (degree), and the symbol corresponds to 25 flights. The color-bar range is from 2.39 to 7.9  $\mu\text{Sv/hr}$ , and the color indicates the averaged dose rate. In the graph, three bottom-right flights have a relatively high maximum altitude but low maximum latitude, so consequently have a relatively low mean dose rate. On the other way, the leftmost flight has a relatively high maximum latitude but low maximum altitude, so it has a relatively low mean dose rate. Likewise, flights with somewhat high maximum altitude and latitude could reach a relatively high mean dose rate. This interpretation is coincident with the previous result of Ahn et al. (2020). However, we know there is a limitation in this rough interpretation because it is just a simple comparison between maximum altitude and maximum latitude with a

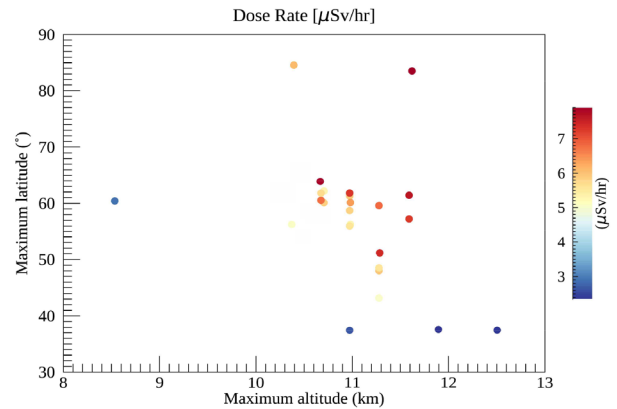


Fig. 1. Averaged effective dose rate with maximum altitude and maximum latitude for a total of 25 flights.

mean dose rate. Even we do not consider the longitudinal effect. It is crucial because it is relevant to the geomagnetic cutoff rigidity, which is the critical factor indicating how well the Earth's geomagnetic field shield the solar wind charged particles by deflecting them back to space, varying with both the latitude and the longitude. It could be improved if we can obtain precise air route information, including the altitude, the latitude, and the longitude. For this purpose, GPS equipment should be accompanied by radiation measurement. We remain more complemented experiments for future work.

### 3.2 Comparison between Liulin-6K Data and KREAM Model

We calculated the effective dose using KREAM for the identical 25 flights. Fig. 2 shows the comparison between Liulin observations (green) and KREAM model results (red) for three return flights to ICN. Fig. 2(a), 2(b), and 2(c) are the plots for the return flights to ICN from ATL, FRA, and SGN, respectively. They are typical examples of frequently used air routes of North America, Europe, and Southeast Asia. In Fig. 2(a) and 2(b), the effective dose rates suddenly drop when the aircraft arrives above the airport, even though they still keep their altitude. This might be due to the cutoff rigidity effect. The cutoff rigidity of the area covering ICN is from 5 to 10 GV. It differs so much from that of ATL and FRA, whose amount is about 1 to 5 GV. It means that areas with ATL and FRA are relatively vulnerable to precipitating charged particles of the solar wind. Although the cutoff rigidity is over 10 GV, which is relatively high, as Fig. 2(c) shows that there might be some attenuation of impact of the cutoff rigidity on the effective dose rate when it rises over a certain range in flight altitude.

Table 3 describes the total effective dose of *in-situ* data from Liulin equipment and model values from three

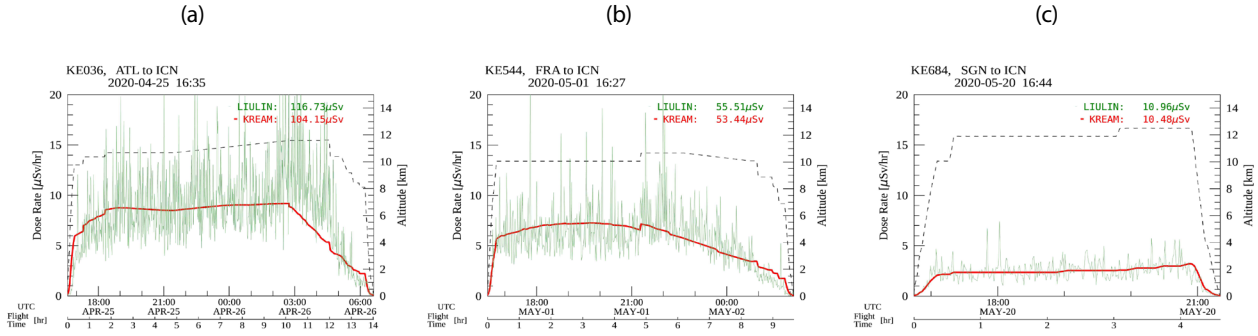


**Fig. 2.** Comparison between Liulin observation data (green) and KREAM result (red) for three return flights. Dashed lines indicate the altitude profile (black). (a) April 25, 2020, ATL–ICN, (b) May 1, 2020, FRA–ICN, (c) May 20<sup>th</sup>, 2020, SGN–ICN.

**Table 3.** Comparison between Liulin observation data and prediction model data of NAIRAS, CARI-6M, and KREAM

	Liulin-6K (A) (μSv)	NAIRAS (B) (μSv)	Error(% , 100× ((B-A)/A))	CARI-6M (C) (μSv)	Error (% , 100× ((C-A)/A))	KREAM (D) (μSv)	Error (% , 100× ((D-A)/A))
1	61.32	101.09	64.86	68.75	12.12	56.87	-7.26
2	56.50	98.61	74.53	67.24	19.01	51.01	-9.72
3	102.82	137.25	33.49	82.49	-19.77	76.25	-25.84
4	84.00	120.63	43.61	70.96	-15.52	84.78	0.93
5	80.60	-	-	-	-	71.26	-11.59
6	81.79	121.02	47.96	69.70	-14.78	80.53	-1.54
7	52.44	101.09	92.77	68.75	31.10	49.82	-5.00
8	6.10	-	-	-	-	7.87	29.02
9	47.18	66.18	40.27	44.62	-5.43	46.77	-0.87
10	25.19	23.20	-7.90	27.44	8.93	23.88	-5.20
11	54.36	42.87	-21.14	31.93	-41.26	44.72	-17.73
12	70.72	120.69	70.66	72.74	2.86	62.31	-11.89
13	95.65	120.35	25.82	52.91	-44.68	75.14	-21.44
14	116.73	131.86	12.96	71.55	-38.70	104.15	-10.78
15	55.59	73.41	32.06	53.37	-3.99	47.18	-15.13
16	15.46	-	-	-	-	15.49	0.19
17	55.51	98.61	77.64	67.24	21.13	53.44	-3.73
18	62.04	42.87	-30.90	31.93	-48.53	48.39	-22.00
19	90.05	120.69	34.03	72.74	-19.22	72.31	-19.70
20	83.95	101.09	20.42	68.75	-18.11	71.18	-15.21
21	67.87	98.61	45.29	67.24	-0.93	57.07	-15.91
22	11.16	5.85	-47.58	13.28	19.00	10.28	-7.89
23	10.96	6.29	-42.61	16.82	53.47	10.48	-4.38
24	75.50	137.25	81.79	82.49	9.26	74.90	-0.79
25	113.73	120.63	6.07	70.96	-37.61	102.31	-10.04
Average error			43.38		22.06		10.95

different models of NAIRAS, CARI-6M, and KREAM, and shows their percent error between observational data and model run results. The top plot of Fig. 3 shows the total effective dose distribution, and the bottom plot shows their percent error distribution. As shown in Fig. 3, NAIRAS (green) results are located higher than all the other models, and observation data and KREAM (red) produces the most similar values with Liulin data (purple). CARI-6M (blue) seems to be located in the lowest region. This tendency becomes the absolute percent error in the bottom panel in Fig. 3. KREAM’s percent error (red) is distributed near the

zero lines, and that of CARI-6M spreads out more widely. This spread is most severe in NAIRAS’s percent error (green). The formula to obtain a percent error is as follows.

$$\text{Percent error} = \left( \frac{\text{Model value} - \text{Liulin value}}{\text{Liulin value}} \right) \times 100$$

Consequently, KREAM values show the lowest error in 19 cases out of 25 cases, while CARI-6M and NAIRAS are closest to Liulin value in five cases and only one case, respectively.

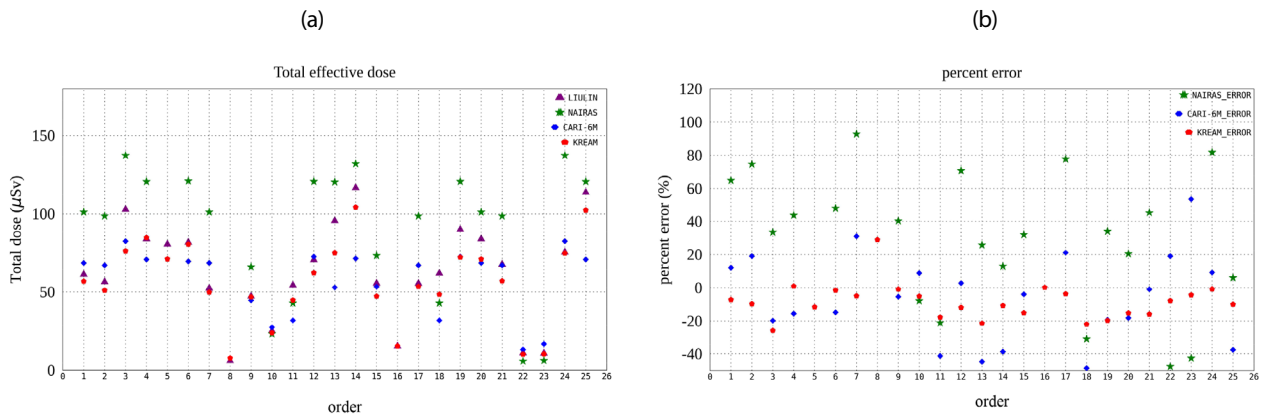


**Fig. 3.** (a) comparison of total effective dose for 25 flights between Liulin data and three different models of NAIRAS, CARI-6M, and KREAM, (b) percent error (%) between observation and each model.

KREAM values show over 20% error in just 4 cases, and the maximum error is 29%, which is under 30%. The number of 30% is critically important because the acceptance level of uncertainty in the radiation estimation program should be 30%, as suggested by the Korea Institute of Nuclear Safety (KINS). In the case of CARI-6M, the error exceeds 40% error in 4 cases, it is located between 20% and 40% in 4 cases, and the maximum error is even 53.5%. In the case of NAIRAS, the error exceeds 60% in 6 cases, it is located between 40% and 60% in 6 cases, which is between 20% and 40% in 7 times, and their maximum error is 92.3% surprising. The averaged errors are 43.38%, 22.03%, and 10.95% for NAIRAS, CARI-6M, and KREAM, respectively. NAIRAS cannot satisfy the acceptance level of uncertainty while CARI-6M and KREAM satisfy that criteria. At the bottom of Fig. 3, the error over 0 means model values exceeds *in-situ* data, and vice versa as a whole, NAIRAS values are higher than Liulin data except 5 cases. In the case of CARI-6M, the values fluctuate up and down around Liulin data, while KREAM values tend to have a little lower value than Liulin data except for 3 cases. Also, as shown in the bottom of Fig. 3, the tendency of the fluctuation of the KREAM value is most similar to that of the Liulin data. It is more important than difference of the values itself, because values which are less than the 30% ICRU/ICRP criterion for dose assessments at aviation altitude can be acceptable (ICRU 2010).

We might interpret why KREAM shows slightly lower values than Liulin data from the uncertainty of both KREAM GPS data and Liulin data. KREAM activates how it temporally produces global dose map first based on GCR and SEP input spectrum and calculates a spatial summation of the effective doses of locations where the aircraft passed. However, some missing data points of locations are extrapolated within known neighborhood data points. Such extrapolation might cause underestimation of radiation

exposure calculation of KREAM. We analyzed dose from spatially intact flight route for some flights and confirm that this underestimation somewhat decreases. To solve this problem, we plan to accompany the GPS equipment in the upcoming experiments. Another possibility is due to the uncertainty of Liulin observation itself. In principle, Liulin detects the charged particle only, actually just electrons. It assumes the other particles' fixed contribution in the aircraft altitude, and that method might sometimes cause overestimation of the real radiation exposure.

### 3.3 Radiation Exposure Over the Polar Route in a Solar Minimum

In our research, only two experiments corresponding to the 4th and 14th in Table 3 are carried out over the polar route to ICN from JFK and ATL. Fig. 4 shows the airways of these two polar flights. Black lines indicate the altitude observation data are missing but we can obtain those from the flightaware website. If we cannot obtain the GPS information both measurement and website, it is indicated as white dotted lines as shown at the bottom of Fig. 4. The 14th flight has too high maximum latitude and maximum altitude, which leads to the highest route dose and mean dose rate among a total of 25 flights, whose amounts are 116.72  $\mu\text{Sv}$ , and 7.9  $\mu\text{Sv/hr}$ , respectively. For the 4th flight (Polar 1 in Fig. 5), the mean dose rate is not so high as 6.1  $\mu\text{Sv/hr}$  even though the polar route. This might be based on the low maximum altitude of 10.39 km. This is the lowest among all experiments over North-America.

Although both the 4th and 25th flight in Table 1 identically took off from JFK and landed on ICN, the 4th flight used the polar route, and the 25th flight did not. In this case, the 4th flight saved about an hour of flight time, and whose route dose and mean dose rate are lower than those of the

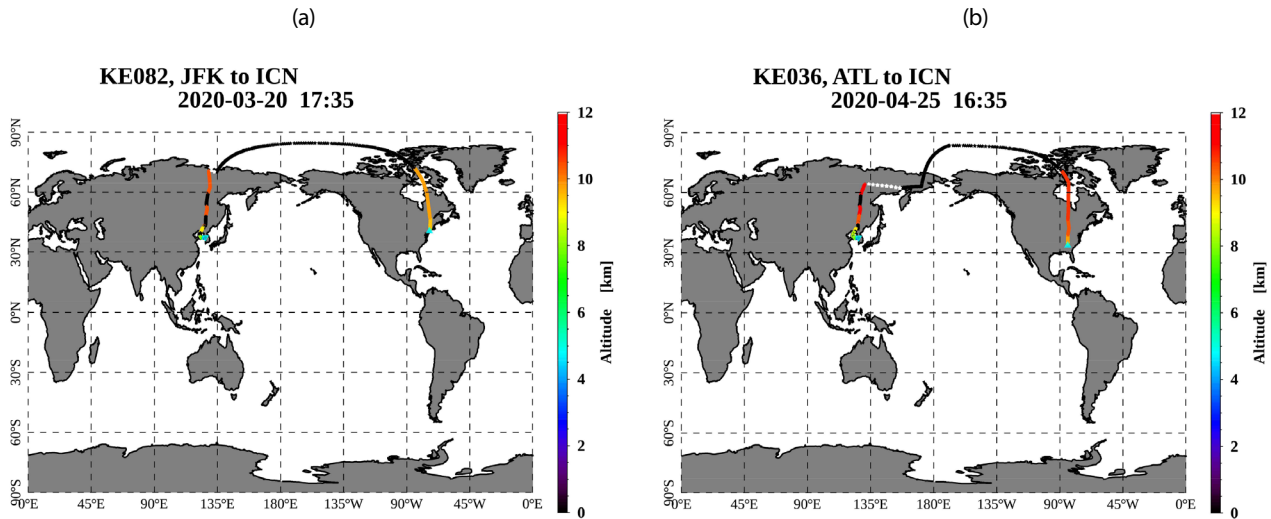


Fig. 4. Flight routes over the polar route corresponding to the 4<sup>th</sup> (a) and the 14<sup>th</sup> (b) are in Table 3. The color indicates an altitude, and the black line indicates the extrapolated altitude profile due to missing data.

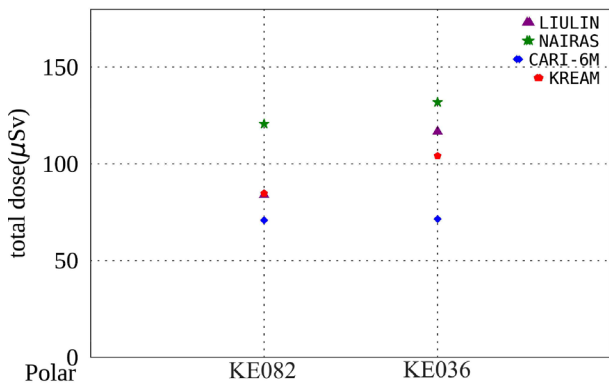


Fig. 5. Comparison between Liulin data and three models of NAIRAS CARI-6Mm and KREAM for two polar routes corresponding to the flights of Fig. 4.

other flight. It also can be concluded that the altitude plays a significant role in this difference because the maximum altitude of the 25th flight is about 11.59 km, which is the second-largest maximum altitude. And flight time is also an essential factor. The 25th flight takes one hour longer than the 4th flight, and it might cause the more significant route dose of the 25th flight. By this comparison, we can conclude that aircrew and passengers should pay careful attention to the altitude changes during their voyager over the polar route even though a solar event was not predicted. Suppose solar events occur during the flight over the polar route. In that case, there could be a much dramatic increase because many high-energy charged particles (especially protons) might precipitate into the polar region (Mertens et al. 2010).

Fig. 5 shows the comparison plot of two polar routes separated from Fig. 3(a). In the case of polar 1 (the 4th in Fig. 3),

the KREAM value is very similar to Liulin data because flight route data is linear, as shown in the upper panel of Fig. 4. On the other hand, the KREAM value of polar 2 (the 14th in Fig. 3) is comparatively lower than the Liulin value, which might be because there is missing data around longitude of 140°E as shown in the bottom panel of Fig. 4. The values of Liulin and KREAM are comparatively higher than those of CARI-6M on both flights. NAIRAS values are much higher than Liulin data. It is clear that there is a general tendency; NAIRAS produces the highest values, Liulin/KREAM has median values, and CARI-6M makes the lowest values.

#### 4. SUMMARY AND CONCLUSION

Recently the necessity of precise prediction and measurements of aviation radiation is increasing in Korea. Several radiation prediction models exist in aircraft altitudes such as NAIRAS, CARI-6/6M, Sievert, EPCARD, JISCARD, PCaire, etc. For our air crew and passengers' radiation safety, we develop our radiation prediction model, KREAM. In this paper, we validate the KREAM model based on comparison with Liulin observations. We perform 25 experiments to measure aviation radiation exposure using Liulin-6K for the early three months of this year. We found that KREAM's result is very well consistent with Liulin observation. NAIRAS is mostly higher than Liulin observation, while CARI-6M is generally lower than observation. The percent error of KREAM compared with Liulin observation is 10.95%. That is 43.38% for NAIRAS and 22.03% for CARI-6M. We found that the increase of the

altitude might cause sudden increase in radiation exposure, especially for the polar route. As more comprehensive analysis is required to validate KREAM's reliability, we plan to expand these radiation measurements with Liulin and TEPC in the near future.

## ACKNOWLEDGMENTS

This work was supported by the project "A Study on the Forecasting Model of Space Radiation and the Improvement of Measuring Equipment (200314)", funded by Korea Foundation of Nuclear Safety.

## ORCID

Junga Hwang <https://orcid.org/0000-0002-6862-5854>  
Jaeyoung Kwak <https://orcid.org/0000-0001-7143-551X>  
Gyeongbok Jo <https://orcid.org/0000-0003-4366-1143>  
Uk-won Nam <https://orcid.org/0000-0003-2398-1019>

## REFERENCES

- Ahn HB, Kim KW, Choi YC, A study on the reduction of cosmic radiation exposure by flight crew, *J. Korean Soc. Aviat. Aeronaut.* 28, 1-6 (2020). <https://doi.org/10.12985/ksaa.2020.28.1.001>
- Dachev TP, Semkova JV, Tomov BT, Matviichuk YN, Dimitrov PG, et al., Overview of the Liulin type instruments for space radiation measurement and their scientific results, *Life Sci. Space Res.* 4, 92-114 (2015). <https://doi.org/10.1016/j.lssr.2015.01.005>
- Green AR, Bennett LGI, Lewis BJ, Kitching F, McCall MJ, et al., An empirical approach to the measurement of the cosmic radiation field at jet aircraft altitudes, *Adv. Space Res.* 36, 1618-1626 (2005). <https://doi.org/10.1016/j.asr.2005.03.061>
- Hwang J, Dokgo K, Choi E, Park JS, Kim KC, et al., Modeling of space radiation exposure estimation program for pilots, crew and passengers on commercial flights, *J. Astron. Space Sci.* 31, 25-31 (2014). <https://doi.org/10.5140/JASS.2014.31.1.25>
- Hwang J, Lee J, Cho KS, Choi HS, Rho S, et al., Space radiation measurement on the polar route onboard the Korean commercial flights, *J. Astron. Space Sci.* 27, 43-54 (2010). <https://doi.org/10.5140/JASS.2010.27.1.043>
- ICRU, Reference data for the validation of doses from cosmic-radiation exposure of aircraft crew, International Commission on Radiation Units and Measurements, ICRU Rep. 84 (2010).
- Irvine EA, Shine KP, Stringer MA, What are the implications of climate change for trans-Atlantic aircraft routing and flight time?, *Transp. Res. D Transp. Environ.* 47, 44-53 (2016). <https://doi.org/10.1016/j.trd.2016.04.014>
- Kubančák J, Ambrožová I, Ploc O, Pachnerová Brabcová K, Štěpán V, et al., Measurement of dose equivalent distribution onboard commercial jet aircraft, *Radiat. Prot. Dosimetr.* 162, 215-219 (2014). <https://doi.org/10.1093/rpd/nct331>
- Malimban J, Nam UW, Pyo J, Youn S, Ye SJ, Characterization of a new tissue equivalent proportional counter for dosimetry of neutron and photon fields: comparison of measurements and Monte Carlo simulations, *Phys. Med. Biol.* 64, 17NT02 (2019). <https://doi.org/10.1088/1361-6560/ab2f1f>
- Mertens CJ, Kress BT, Wiltberger M, Blattnig SR, Slaba TS, et al., Geomagnetic influence on aircraft radiation exposure during a solar energetic particle event in October 2003, *Space Weather.* 8, S03006 (2010). <http://doi:10.1029/2009SW000487>
- Mertens CJ, Meier MM, Brown S, Norman RB, Xu X, NAIAS aircraft radiation model development, dose climatology, and initial validation, *Space Weather.* 11, 603-635 (2013). <https://doi.org/10.1002/swe.20100>
- O'Brien K, Smart DE, Shea MA, Felsberger E, Schrewe U, et al., World-wide radiation dosage calculations for air crew members, *Adv. Space Res.* 31, 835-840 (2003). [https://doi.org/10.1016/S0273-1177\(02\)00882-7](https://doi.org/10.1016/S0273-1177(02)00882-7)
- Ploc O, Pachnerová Brabcová K, Spurný F, Malušek A, Dachev T, Use of energy deposition spectrometer Liulin for individual monitoring of aircrew, *Radiat. Prot. Dosimetr.* 144, 611-614 (2011). <https://doi.org/10.1093/rpd/ncq505>
- Spurný F, Response of a Si-diode-based device to fast neutrons, *Radiat. Meas.* 39, 219-223 (2005). <https://doi.org/10.1016/j.radmeas.2004.05.006>
- Wilson JW, Mertens CJ, Goldhagen P, Friedberg W, De Angelis G, et al., Atmospheric ionizing radiation and human exposure, NASA Technical Publication, NASA/TP-2005-213935 (2005).